SF2A 2025
A. Siebert, K. Baillié, M. Béthermin, F. Cantalloube, E. Josselin, N. Lagarde, J. Malzac, J. Richard, L. Selliez, O. Venot (eds)

FAILED QUENCHING IN MASSIVE SPIRAL GALAXIES

R. Cologni[1,2], P. Salomé[1], D. Le Borgne[2], P. Guillard[2], M. Boquien[3], S. Flesch[1], L. Bouscasse[4] and F. Combes[1]

Abstract. Recent studies highlighted the existence of a population of extended and actively star forming spiral galaxies in a mass range almost entirely populated by elliptical and quenched galaxies ($M_\star > 10^{11} M_\odot$). These objets are of great interest because they challenge mass-quenching scenarios, and therefore question our knowledge on galaxy evolution. We know that mass accretion can severely affect both the rotation-supported disc shape and star formation (SF) activity, either by disrupting the gas and stellar dynamics (mergers, collisions) or by depriving the galaxy of its gas content (RAM pressure stripping, tidal effects, AGN feedback). However, SSGs have preserved both their spiral morphology and a standard / high star formation rate (SFR) throughout their growth process. As such, SSGs constitute a relevant population to study failed quenching in galaxies. In this contribution, I will present preliminary results from molecular gas observations (NOEMA/IRAM) of a small sample of SSGs at redshift $z \sim [0.01 ; 0.25]$, which allows us to map the distribution of their cold gas reservoir. I will then explain the methods developed using SED fitting to measure the resolved star-formation efficiency for one of them.

Keywords: galaxies: evolution – galaxies: ISM – galaxies: spirals – galaxies: star formation

1 Introduction

The population of galaxies in the high-mass range ($M_\star > 10^{11} M_\odot$) is virtually entirely represented by quenched early-type galaxies. Except for 6 % of the most luminous galaxies observed by Ogle et al. (2016, 2019b) at redshift $z < 0.3$, that are indeed massive super spiral galaxies (SSG). 84 SSGs have been cataloged in the Ogle Galaxy Catalog* (OGC), alongside super lenticular, and super mergers. Massive spiral galaxies might be the most efficient at accumulating baryons and converting them into stars (Posti et al. 2019; Ogle et al. 2019a). Indeed, they exhibit high baryonic fractions $f_M = M_\star / M_{\mathrm{halo}}$, approaching the cosmological baryon fraction of $f_b = \Omega_b/\Omega_b = 0.188$ (Planck Collaboration et al. 2020). This result is high above what one would expect from the reference stellar-to-halo mass ratio (SHMR) peaking $f_M \simeq 0.2 f_b$ (for L^*), and decreasing both towards the low and high-mass ends. When limiting the scope to spirals, studies show a monotonously increasing $f_\star$ with stellar mass, in place of the expected steep decreasing curve (Di Teodoro et al. 2023), thus reaching nearly a 100% efficiency, i.e. no missing baryons.

Moreover, the star forming rates (SFRs) of the SSGs are ranging 1-80 $M_\odot$ yr^{-1}, which is remarkably high for galaxies located in this mass-range, as the vast majority of galaxies at $M_\star > 10^{11} M_\odot$ are quenched ellipticals. These rates place SSGs on the high-mass end of the star-forming Main Sequence (SFMS), in a regime where mass-quenching is thought to have already taken place, and thus prevented star formation to carry on. The physical processes that in general galaxies undergo as they build their mass (e.g. mergers, AGN feedback) either disturb the gas, driving it to become unfit to form stars, or simply remove it from the galaxy. Surprisingly, SSGs seem to have failed at quenching. Thus, in order to better understand and characterize SF in such objects, it is necessary to probe the interstellar medium (ISM) phase where SF takes place, i.e. their molecular gas. Unresolved detections of CO(1-0) in 46 SSGs with IRAM 30m telescope point towards high molecular gas mass

[1] LUX, Observatoire de Paris, PSL Research University, Sorbonne Université, CNRS, 75014 Paris, France
[2] Sorbonne Université, CNRS, UMR 7095, Institut d'Astrophysique de Paris, 98bis bd Arago, 75014 Paris, France,
[3] Université Côte d'Azur, Observatoire de la Côte d'Azur, CNRS, Laboratoire Lagrange, 06000, Nice, France
[4] IRAM, 300 rue de la Piscine, 38400 Saint-Martin-d'Hères, France
*`https://vizier.cds.unistra.fr/viz-bin/VizieR-3?-source=J/ApJS/243/14/table6`

fraction ($f_{\rm mol} = {\rm M_{H2}}/{\rm M_\star}$), and slightly higher molecular depletion times ($\tau_{\rm dep} = {\rm M_{H2}}/{\rm SFR}$) than the spirals of lower mass, located on the SFMS (Lisenfeld et al. 2023, L23 henceforth).

The two main focuses of this contribution are the following: we present the first resolved CO detection of SSGs obtained with the IRAM/NOEMA interferometer. We then introduce our method to measure spatially-resolved properties is these objects using SED fitting.

2 CO observations

SF occurs in the coldest phase of the ISM: the giant molecular clouds (GMCs). Observing H_2 is of great difficulty, due to the symmetry of the molecule, hence the absence of a dipole moment. Therefore, we indirectly probe molecular gas through the emission of CO molecules, which are also present in GMCs, although less abundantly than H_2. Conversion from CO integrated flux density to H_2-mass was carried out by firstly obtaining the line luminosity $L'_{\rm CO}$ from eq. (3) of Solomon et al. (1997). Hence, we were able to deduce the molecular gas masses following: $M_{\rm mol} = \alpha_{\rm CO} \times L'_{\rm CO}$, where $\alpha_{\rm CO} = 4.3$ $M_\odot$ (K km s^{-1} pc^2)$^{-1}$ is the standard value of molecular gas mass-to-light ratio for the Milky Way (Bolatto et al. 2013).

The sources in the sample were selected according to several criteria, in order to investigate the diverse characteristics of these extreme objects. Not only did we seek actively star-forming galaxies, but we also chose baryon-rich sources from dynamical studies of lower-z massive spirals. Besides, our sample is balanced between passive and active source, allowing us to address the question of failed AGN-feedback in this population of unquenched galaxies.

The observations were carried out with the Institut de Radioastronomie Millimetrique (IRAM) Northern Extended Millimetre Array (NOEMA) interferometer. We obtained resolved detections of molecular gas probed with CO(1-0) emission line in 6 SSGs and 9 lower-z counterparts. Our sample is consequently divided in two redshifts bins. The 6 SSGs were chosen from the OGC as the most star-forming targets and with a redshift of $z < 0.2$, except for OGC 217 ($z = 0.2489$), which is the most star-forming of all SSGs (SFR= 78 $M_\odot$ yr^{-1}, L23). The stellar masses and SFR of this subsample are ranging $M_\star$ = 3.4 - 4.6 $\times 10^{11} M_\odot$ and SFR = 15-77 $M_\odot$ yr^{-1} (L23). In compact configuration, NOEMA allowed us to reach angular resolutions of 1.3"-3.9" ($\sim$ 4.5-12 kpc at $z_{\rm med} = 0.17$) and rms$\sim$ 0.3 Jy km s^{-1}. The other 9 sources were the most baryon-rich targets chosen both from Posti et al. (2019) and Di Teodoro et al. (2023). These sources at $z_{\rm med} = 0.03$ exhibit lower stellar mass and SFR of respective ranges $M_\star$ = 1.4 - 2.3 $\times 10^{11} M_\odot$ and SFR = 1.2 - 19 $M_\odot$ yr^{-1}. The observations reached a rms $\sim$ 0.7 Jy km s^{-1} and an angular resolution of 1.1"-4.9" ($\sim$ 0.7-3 kpc). The data calibration was performed using the standard pipeline in `CLIC`, and the imaging using `MAPPING`, two softwares from the GILDAS[†] package. We smoothed the spectra of native resolution $\sim$ 5km s^{-1} to a spectral resolution of $\sim$ 20 km s^{-1}.

3 Resolved SED fitting method

The resolved detection of molecular gas allows us to derive the spatial distribution of properties such as molecular gas mass fraction $f_{\rm mol}$ or molecular depletion time $\tau_{\rm dep}$ for which no studies have yet been conducted in SSGs. For this purpose, we need a method to estimate SFR and stellar mass in a resolved manner. Given that all sources have been observed in ultraviolet with GALEX (Galaxy Evolution Explorer), in visible by SDSS (Sloan Digital Sky Survey) and in mid-infrared by WISE (Wide-field Infrared Survey Explore), we have access to the necessary and sufficient archival data to perform Spectral Energy Distribution (SED) fitting in sub-regions.

The data come from various instruments and have therefore different angular resolution. Hence, images need to be homogenized to a common Point Spread Function (PSF) beforehand, to avoid any color aberration in the spectra. We performed a convolution on each band to the coarsest resolution, namely that of band 3 of WISE, using high resolution kernels from the Astronomical Convolution-kernel repository[‡]. The convolved images were then reprojected on a common grid of 6 arcsec-wide pixels. One should note that all data have been background subtracted and UV and optical images were corrected for Galactic extinction using the $E(B-V)$ values from NASA/IPAC Infrared Science Archive[§], and following the prescriptions from Schlafly & Finkbeiner (2011).

There exist numerous SED fitting codes relying on various assumptions, among which we chose CIGALE (Boquien et al. 2019, Code Investigating GALaxy Emission) to find the best spectrum fit to each of the pixels,

[†] `http://www.iram.fr/IRAMFR/GILDAS`

[‡] `https://www.astro.princeton.edu/~draine/Kernels/Kernels_2018/Kernel_FITS_Files/Hi_Resolution/`

[§] `https://irsa.ipac.caltech.edu/applications/DUST/`

constrained by 10 photometric fluxes ranging from GALEX-*FUV* (154.8 nm) to *WISE3* (11.4 μm). The basic property on which CIGALE relies is the energy balance between the absorption of the light in the UV and optical range, and its re-emission in the mid- and far-infrared. The module-based architecture of CIGALE allows great flexibility, and easy tailoring of the parameter-space on wishes to explore.

4 Results

4.1 CO detection

For the total of 15 galaxies observed, we clearly detect a rotating disc of molecular gas at the galaxy center, yet with morphological variations from a source to another. An example is shown in Figure 1 for three sources. OGC 543 (middle row) is a barred active galaxy and exhibits a ring in molecular gas, whereas OGC 586 (top row) seem to have a smooth and compact disc of cold gas. As for UGC 8179 (bottom row), the disc appears asymmetrical, and the velocity field visibly points to the existence of a bar, since the kinematic minor axis is not perpendicular to the major axis, which was not clear from optical images.

The measured molecular gas masses are distinctly greater for the subsample of 6 OGC SSGs (M_{H2} = 12.3-87.6 $\times 10^9 M_\odot$) than for the 9 lower-mass, more nearby spirals (M_{H2} = 0.6-6.41 $\times 10^9 M_\odot$). One exception: UGC 8179 that has the best SNR of this subsample, has a molecular gas mass of 24.2 $\times 10^9 M_\odot$, and a remarkably higher SFR than the rest of the targets in this subsample.

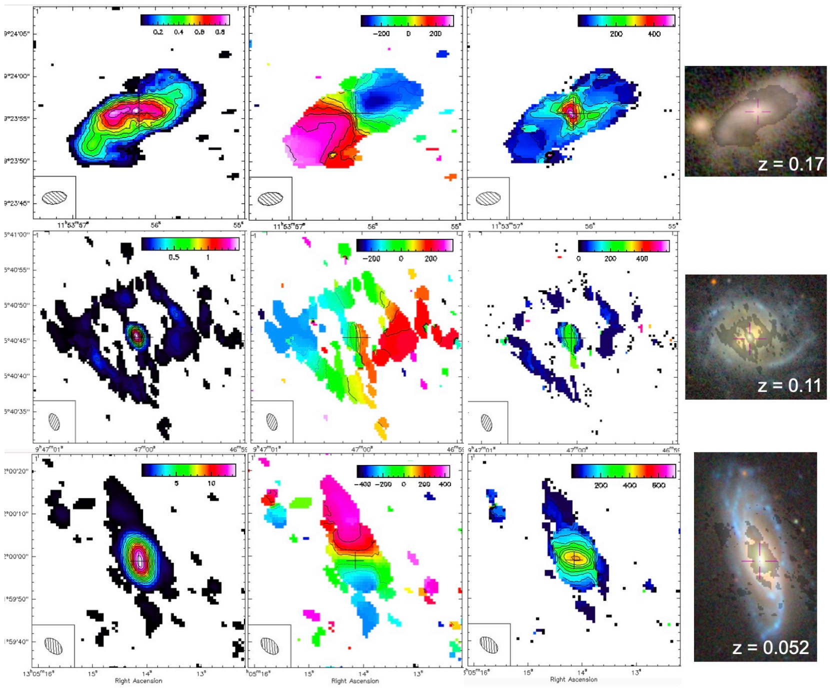

Fig. 1. Moment maps of OGC 586, OGC 543 and UGC 8179 (top to bottom row). **From left to right:** Moment 0 map (integrated intensity in Jy/beam km s^{-1}), moment 1 map (intensity-weighted velocity, in km s^{-1}), moment 2 map (square root of the intensity-weighted velocity dispersion, or line width in km s^{-1}), optical color (i, r, g) image overlayed with moment 0 map.

4.2 Resolved properties

The method described in Section 3 was developed on UGC 8179 (bottom row in Fig 1) and allowed us to visualize the spatial distribution of $f_{\rm mol}$ and $\tau_{\rm dep}$ for the pixels where we detect CO (unhatched pixels in the left and middle panels of Figure 2). For this galaxy at $z = 0.0519$, we are limited by the field of view of NOEMA that doesn't encompass the entire disc. We note a relatively constant $\log_{10} f_{\rm mol} \sim -0.9$ in the central part of the disc, and enhanced star-forming efficiency (SFE=$1/\tau_{\rm dep}$) towards the spiral arms. We show the resolved Kennicutt-Schmidt (rKS) relation in the right panel of Fig. 2, namely SFR surface density with respect to M_{H2} surface density. This graph is a preliminary attempt to answer the question: are the SSGs forming stars at the same efficiency as MS spirals ? For comparison, we included one of the many rKS for nearby MS galaxies, the one of Querejeta et al. (2021) who studied the galaxies from PHANGS (Physics at High Angular resolution in Nearby GalaxieS) sample. One can notice that the resolved data points follow the trend of the standard spirals of PHANGS, although with an offset of roughly 0.3dex towards the larger depletion times.

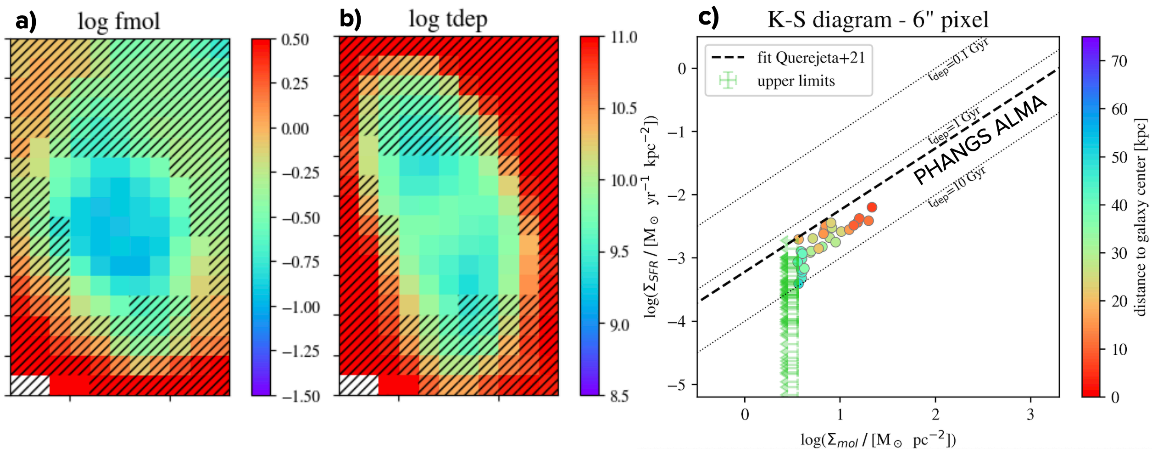

Fig. 2. a): Molecular gas mass fraction map (in decimal log), the hatched pixels are where CO signal is below the detection threshold of 3σ. **b):** Molecular gas depletion time map (in decimal log). **c):** Resolved Kennicutt-Schmidt relation, upper limits in $\Sigma_{\rm mol}$ correspond to the hatched pixels. The dashed black line is the linear fit across all morphological masks in nearby galaxies from PHANGS (Querejeta et al. 2021).

5 Conclusions

We presented the first resolved detections of molecular gas in Super Spiral galaxies and less extreme, yet baryon-rich, nearby massive spiral galaxies. These observations confirm the presence of an important cold gas reservoir and yields the conclusion that molecular gas has not been depleted from these galaxies (e.g. by AGN feedback). It raises the question of the fueling of the reservoir, either by secular accretion or by gas-rich mergers.

We developed a method taking advantage of archival data ranging from UV to mid-infrared, in order to perform resolved SED fitting on one galaxy of the sample. The results show for this one galaxy that depletion times are higher than in regular MS spirals, i.e. lower SFE, which is compatible with the results of L23 from unresolved CO observations. This method will be applied to the entire sample of galaxies for which we have mapped molecular gas (Cologni et al., in prep). This will grant us with more statistically robust conclusions to draw from this resolved method. One limitation of our study is that the field of view for the nearby subsample restrict the CO detection to the inner part of the disc, whereas the entire discs of the 6 OGC galaxies are encompassed in the NOEMA primary beam.

RC thanks the organizers of the SF2A 2025 annual meeting. This paper is based on data obtained using IRAM/NOEMA interferometer, that benefited from the funding from ... The authors would like to thank the IRAM/NOEMA staff for their support during observations, Laure Bouscasse for her help in preparing observation and data reduction, and the IRAM ressources for storage and calibration softwares. The authors would also like to gratefully thank Jonathan Freudlich and Ute Lisenfeld for insightful discussions. The authors benefited from the support of Initiative Physique des Infinis, from Sorbonne Université.

References

Bolatto, A. D., Wolfire, M., & Leroy, A. K. 2013, ARA&A, 51, 207

Boquien, M., Burgarella, D., Roehlly, Y., et al. 2019, A&A, 622, A103

Di Teodoro, E. M., Posti, L., Fall, S. M., et al. 2023, MNRAS, 518, 6340

Lisenfeld, U., Ogle, P. M., Appleton, P. N., Jarrett, T. H., & Moncada-Cuadri, B. M. 2023, A&A, 673, A87

Ogle, P. M., Jarrett, T., Lanz, L., et al. 2019a, ApJ, 884, L11

Ogle, P. M., Lanz, L., Appleton, P. N., & et al. 2019b, The Astrophysical Journal Supplement Series, 243, 14

Ogle, P. M., Lanz, L., Nader, C., & Helou, G. 2016, ApJ, 817, 109

Planck Collaboration, Aghanim, N., Akrami, Y., et al. 2020, Astronomy and Astrophysics, 641, A6

Posti, L., Fraternali, F., & Marasco, A. 2019, A&A, 626, A56

Querejeta, M., Schinnerer, E., Meidt, S., et al. 2021, A&A, 656, A133

Schlafly, E. F. & Finkbeiner, D. P. 2011, ApJ, 737, 103

Solomon, P. M., Downes, D., Radford, S. J. E., & Barrett, J. W. 1997, ApJ, 478, 144